Published in final edited form as:
Biochim Biophys Acta. 2014 December ; 1842(12 0 0): 2517–2527. doi:10.1016/j.bbadis.2013.03.004.

Cyclophilin D deficiency rescues Aβ-impaired PKA/CREB signaling and alleviates synaptic degeneration

Heng Du[a,1], **Lan Guo**[a,1], **Xiaoping Wu**[b], **Alexander A. Sosunov**[b], **Guy M. McKhann**[b], **John Xi Chen**[c], and **Shirley ShiDu Yan**[a,*]

Shirley ShiDu Yan: shidu@ku.edu

[a]Department of Pharmacology and Toxicology, and Higuchi Bioscience Center, School of Pharmacy, University of Kansas, Lawrence, KS 66047, USA

[b]Department of Neurosurgery, Physicians & Surgeons College of Columbia University, New York, NY 10032, USA

[c]Department of Neurology, Memorial Sloan-Kettering Cancer Center, New York, NY 1003, USA

Abstract

The coexistence of neuronal mitochondrial pathology and synaptic dysfunction is an early pathological feature of Alzheimer's disease (AD). Cyclophilin D (CypD), an integral part of mitochondrial permeability transition pore (mPTP), is involved in amyloid beta (Aβ)-instigated mitochondrial dysfunction. Blockade of CypD prevents Aβ-induced mitochondrial malfunction and the consequent cognitive impairments. Here, we showed the elimination of reactive oxygen species (ROS) by antioxidants probucol or superoxide dismutase (SOD)/catalase blocks Aβ-mediated inactivation of protein kinase A (PKA)/cAMP regulatory-element-binding (CREB) signal transduction pathway and loss of synapse, suggesting the detrimental effects of oxidative stress on neuronal PKA/CREB activity. Notably, neurons lacking CypD significantly attenuate Aβ-induced ROS. Consequently, CypD-deficient neurons are resistant to Aβ-disrupted PKA/CREB signaling by increased PKA activity, phosphorylation of PKA catalytic subunit (PKA C), and CREB. In parallel, lack of CypD protects neurons from Aβ-induced loss of synapses and synaptic dysfunction. Furthermore, compared to the mAPP mice, CypD-deficient mAPP mice reveal less inactivation of PKA–CREB activity and increased synaptic density, attenuate abnormalities in dendritic spine maturation, and improve spontaneous synaptic activity. These findings provide new insights into a mechanism in the crosstalk between the CypD-dependent mitochondrial oxidative stress and signaling cascade, leading to synaptic injury, functioning through the PKA/CREB signal transduction pathway.

*Corresponding author at: Department of Pharmacology and Toxicology and Higuchi Bioscience Center, Schoolof Pharmacy, University ofKansas, 2099 constant Ave. Lawrence, KS 66047, USA. Tel.: +1 785 864 3637.
[1]Authors contribute equally to this work.

Conflict of interest: The authors have no conflict of interest to disclose.

Appendix A. Supplementary data: Supplementary data to this article can be found online at http://dx.doi.org/10.1016/j.bbadis.2013.03.004.

Keywords

Alzheimer's disease; Amyloid beta; Mitochondrial permeability transition; Synaptic alteration; PKA/CREB signaling; Oxidative stress

1. Introduction

Alzheimer's disease (AD) is a chronic neurodegenerative disease characterized by progressive learning and memory deficits [1,2]. Synaptic failure is an early neuropathological hallmark in AD patients and AD animal models. The cognitive decline in AD is closely correlated to pathological synaptic changes, suggesting that synaptic distress is an underlying factor in AD pathogenesis [3,4]. Occurring along with synaptic failure, brain mitochondrial dysfunction is also an early pathology in AD. Human AD and AD animal models demonstrate mitochondrial pathologies including respiration deficits, increased generation/accumulation of free radicals, impaired energy metabolism [5–13], change in mitochondrial dynamics [14–18], and compromised calcium buffer capacity [19,20]. Recent studies highlighted the significance of mitochondrial Aβ accumulation [5,7,8,11,19,21–23]. The coexistence of mitochondrial alterations with synaptic perturbation warrants investigation of a link between synaptic failure and mitochondrial pathology in AD.

Cyclophilin D, a key component of mitochondrial permeability transition pore (mPTP), plays an integral role in Aβ-induced mitochondrial and synaptic injury [19,24,25]. However, the effect of CypD on Aβ-mediated cell signaling cascades controlling synaptic plasticity and activity has not been elucidated.

The PKA/CREB signal pathway acts as a key regulator of synaptic plasticity and learning memory [26–31]. PKA/CREB signaling cascade is affected in Aβ-rich environment leading to dendritic spine architecture change in an AD mouse model [32], suggesting the deleterious role of PKA/CREB disturbances in synaptic alteration in AD. To date, there is no report on the effects of CypD-mediated perturbations on Aβ-induced disruption of PKA/CREB pathway. Thus, it is essential to determine whether CypD-dependent regulation of mitochondrial signal transduction mechanisms via disrupted PKA/CREB signal pathway contributes to Aβ-induced synaptic injury.

The present study addresses the key questions noted here and elucidates new insights into mechanisms underlying CypD and Aβ-induced damage to synaptic structure and function, focusing on synaptic structure, oxidative stress, dendritic spine alternations, synaptic activity, and PKA/CREB-associated signal transduction and synaptic function.

2. Methods

2.1. Mice

Animal studies were approved by the Animal Care and Use Committee of University of Kansas in accordance with the National Institutes of Health guidelines for animal care. Transgenic mice expressing a mutant form of the human amyloid protein precursor (APP)

bearing both the Swedish (K670N/M671L) and the Indiana (V717F) mutations (J-20 line) [33], were crossed with *Ppif*$^{-/-}$ mice to generate CypD-deficient mAPP mice (mAPP/*Ppif*$^{-/-}$). Offspring of Tg mice were identified by PCR using primers for each specific transgene as previously described [19]. Twelve month old mice of either sex were used for the study.

2.1.1. Neuronal culture

Primary neuronal cultures were previously described [19]. Primary neurons were maintained in culture for 14 days before treatment. Neurons were incubated with probucol (10 μM) or superoxide dismutases (SOD, 200 U/ml)/Catalase (250 U/ml) for 30 min prior to the addition of Aβ (5 μM) for 2 h.

2.2. Measurement of PKA kinase activity

Mice cortical tissues or cultured neurons were lysed with extraction buffer (10 mM Tris–HCl pH 7.4,100 mM sodium chloride, 1 mMEDTA, 1 mM EGTA, 1 mM sodium fluoride, 20 mM sodium pyrophosphate, 2 mM sodium orthovanadate, 1% Triton X-100,10% glycerol, 0.1% SDS, 0.5% deoxycholate, 1 mM PMSF) containing protease inhibitor cocktail (Calbiochem, set V, EDTA free) and homogenized on ice. Proper amount of samples was added and the levels of intracellular PKA kinase activity were measured by PKA Kinase Activity Assay Kit (Assay Designs) according to manufacturer's instructions.

2.3. Preparation of oligomeric Aβ1–42

Oligomeric Aβ1-42 was prepared from synthetic Aβ1-42, as previously described [19,34]. Oligomeric composition of Aβ1-42 solution was characterized by mass spectrometry.

2.4. Immunoblotting analysis

Mice cortical tissues or cultured neurons were homogenized in extraction buffer (10 mM Tris–HCl pH 7.4, 100 mM sodium chloride, 1 mM EDTA, 1 mM EGTA, 1 mM sodium fluoride, 20 mM sodium pyrophosphate, 2 mM sodium orthovanadate, 1% Triton X-100, 10% glycerol, 0.1% SDS, 0.5% deoxycholate, 1 mM PMSF) containing protease inhibitor cocktail (Calbiochem, set V, EDTA free). After centrifugation at 13,000 rpm at 4 °C, an equal amount of supernatant proteins was subjected to the immunoblotting with the following primary antibodies: mouse anti-phospho (ser133)-CREB IgG (Cell Signaling Technology), rabbit anti CREB IgG (Cell Signaling Technology), rabbit anti phospho (Thr197)-PKA C IgG (Cell Signaling Technology), mouse anti-PKA C IgG (BD Biosciences Pharmingen), rabbit anti-synaptophysin (Dako), mouse anti-α-Tubulin (Sigma). The immunoantigen was detected by goat anti-mouse or rabbit IgG conjugated with horseradish peroxidase (Sigma). We used NIH Image-J computer program for the quantification of the intensity of the immunoreactive bands.

2.4.1. Phosphorylated CREB and total CREB determination—The levels of phospho (Ser133)-CREB were measured after 10 min of exposure to 50 μM glutamate of neurons, which were pretreated with either 5 μM oligomeric Aβ1–42 alone or co-incubation of oligomeric Aβ1–42 with 3 μM rolipram or 5 μM forskolin. Rolipram or forskolin was

added 30 min before the addition of Aβ1–42. After 2 h Aβ1–42 preincubation, the culture medium was replaced by glutamate buffer (20 mM Hepes, 119 mM NaCl, 5 mM KCl, 2 mM $CaCl_2$, 1 μM Glycine, 300 μM Glucose, 50 μM Glutamate). The osmolarity of glutamate buffer was adjusted to 325 mOsm by using sucrose, and pH was adjusted to 7.3 with 10 N NaOH. Cortical tissues or cultured neurons were homogenized in extraction buffer containing protease inhibitor cocktail. The levels of phospho-CREB and total-CREB in neuron were detected by immunoblotting and the levels in mice brain were determined by Enzyme-linked immunosorbent assay (ELISA) according to the manufacturer's instructions (Invitrogen).

2.5. MitoSox Red staining and flow cytometry assay

Neurons were exposed to 0.5 μM MitoSox Red (Invitrogen) for 30 min. After the staining, the culture medium was changed and neurons were kept in an incubator (5% CO_2, 37 °C) for 20 min. Afterwards, neurons were trypsinized from the plates and subjected to flow cytometry (Becton Dickinson FACS Calibur) assay. The flow cytometric data were analyzed by Flowjo 7 (Tree Star). Unstained cells (no MitoSox red staining) were used as a control to detect the specific MitoSox signal. Gates to determine percent of MitoSox-positive cells were set to exclude unstained control cells [35].

2.6. Neuronal synaptic density

Synaptic density of cultured neurons was measured by counting synaptophysin clusters attaching to neuronal dendrites and presented as the number of synaptophysin clusters per micron of dendrite. Neurons were fixed in 4% paraformaldehyde for 20 min and then blocked in 10% goat serum for 30 min. Synaptophysin was visualized by rabbit anti-synaptophysin IgG (Dako) followed by goat anti-rabbit IgG conjugated with TRICT (Sigma-Aldrich Corp.). Neuronal dendrites were visualized by mouse anti-MAP2 IgG (Boehringer Mannheim) followed by goat anti-mouse IgG conjugated with FITC (Sigma-Aldrich Corp.). Images were taken under a Biorad confocal and analyzed by NIH Image J program.

2.7. Electrophysiology

Brain slices were prepared from 12-month-old mice. Mice brain was sliced in ice-cold oxygen modified artificial cerebrospinal fluid (ACSF, 125 mM NaCl, 2.5 mM KCl, 2 mM $CaCl_2$, 1.5 mM $MgCl_2$, 26 mM $NaHCO_3$ and 10 mM glucose). Brain slices were then recovered in ACSF for 60 min at 32 °C. 1 μM tetrodotoxin was added to the bath while patch recording. Whole-cell recording was conducted on pyramidal neurons in hippocampal CA1 region. The patch pipettes were filled with intracellular solution containing 115 mM cesium methanesulfonate, 20 mM CsCl, 10 mM HEPES, 2.5 mM $MgCl_2$, 10 mM sodium phosphocreatine, 4 mM Na_2ATP, 0.4 mM Na_3ATP and 0.6 mM EGTA, pH 7.3. The spontaneous miniature excitatory postsynaptic currents (mEPSCs) were recorded by using MultiClamp 700A (Axon Instrument) and the events were analyzed using Axon clampfit (Axon Instrument, version 8.2.0.235).

2.8. Dendritic spine density and morphology measurements in vivo

CA1 neurons from mice brain slices were microinjected by using patch pipettes filled with intracellular solution as described above containing 0.1% Lucifer yellow CH (Sigma-Aldrich Corp.). Spines on basal dendrites of CA1 neurons were visualized by rabbit anti-Lucifer yellow Ig G (Sigma-Aldrich Corp.) followed by goat anti-rabbit IgG Alexa 488 (Invitrogen). Images were taken under a Biorad confocal and Z stacks were gathered at 0.2 μm increments. The types of spines were recognized based on the measurements. Spines were defined as stubby type if they had a length to neck diameter ratio less than 2. Spines with a length to neck diameter ratio more than 2 were categorized as mushroom type if the ratio of head to neck diameter more than 1.3 fold or thin spines if the ratio of head to neck diameter was less than 1.3 fold [36]. Data were analyzed by using Axiovision LE (Zeiss) software. Analysis of synaptic density and morphology was performed by an investigator blinded to mice genotypes.

2.9. Statistical analysis

We performed statistical analyses with Student's t-test and one-way analysis of variance (ANOVA) as well as post-hoc ANOVA (Tukey's) using the Statview statistics software when appropriate. $P < 0.05$ was considered significant. All data are expressed as means ± s.e.m.

3. Results

3.1. Aβ disturbs PKA/CREB signaling transduction pathway through oxidative stress

PKA activity significantly relies on PKA catalytic subunit (PKA C) phosphorylation on its Thr197 site, which is an integral part in PKA/CREB signal transduction pathway. Given that reactive oxygen species (ROS) is a determined factor for disturbing PKA C Thr197 phosphorylation [37] and that Aβ is a known strong inducer of ROS production, we determine whether Aβ disturbs PKA/CREB signaling transduction through oxidative stress. To evaluate the effects of oxidative stress on Aβ-impaired PKA/CREB signaling cascades, we employed antioxidant probucol or SOD/catalase to extinguish extracellular as well as intracellular ROS as described in our previous studies [19,38,39]. Neurons were incubated with antioxidant probucol or SOD/catalase for 30 min prior to the addition of Aβ for 2 h. Aβ treatment significantly inhibited PKA C phosphorylation (Fig. 1A) and PKA activity (Fig. 1B), while probucol or SOD/catalase treatment protected against Aβ-induced deleterious effects on PKA C phosphorylation and PKA activity (Fig.1A–B). Since CREB is a downstream target of PKA regulation, we extended our study by assessing CREB phosphorylation (pCREB) in response to glutamate stimulation. Glutamate is a strong mediator of CREB activation and previous study showed that glutamate-stimulated CREB phosphorylation is associated with PKA activity [40]. Our results showed that the application of probucol or SOD/catalase significantly reversed Aβ-reduced CREB phosphorylation (pCREB) (Fig. 1C1–C2). Probucol or SOD/catalase alone (without Aβ) had no effects on the baselines of p-PKA C levels, PKA activity or pCREB (Fig. 1A–C2). These data suggest that Aβ-associated oxidative stress is involved in PKA/CREB perturbations in Aβ-insulted neurons.

3.2. CypD deficiency attenuates Aβ-induced mitochondrial ROS production and restores Aβ-perturbed PKA/CREB signaling transduction pathway in vitro

Previous studies have demonstrated that CypD-mediated mitochon-drial permeability transition pore (mPTP) is a critical mechanism underlying Aβ-induced mitochondrial and intracellular oxidative stress in Aβ-insulted neurons. We then performed studies to determine if CypD-mediated mitochondrial ROS is associated with Aβ-disrupted PKA activity. First, cultured nonTg and *Ppif*$^{-/-}$ neurons were exposed to Aβ and subjected to the detection of mitochondrial ROS production by employing MitoSox Red, a specific mitochondrial ROS indicator using flow cytometry. NonTg neurons showed substantially higher percentage of cells positive for MitoSox Red staining than *Ppif*$^{-/-}$ neurons (36.36 ± 1.41% versus 22.75 ± 0.7% in gated area, Fig. 2A) at the exposure to Aβ. There's nosignificant difference in the percentage of MitoSox Red positive cells between nonTg and *Ppif*$^{-/-}$ vehicle-treatment groups. Furthermore, we employed cyclosporine A (CsA), a pharmacological inhibitor for blocking CypD activity. NonTg neurons were pre-exposed to 5 μM CsA or vehicle (no CsA) for 1 h before the co-incubation with Aβ for 2 h, and then subjected to MitoSox Red staining. Aβ-treated nonTg neuronal mitochondria demonstrated significantly decreased MitoSox Red staining intensity in the presence of CsA, suggesting the application of CsA substantially suppressed Aβ-induced mitochondrial ROS elevation (Fig. 2B. Aβ-treatment vs. CsA and Aβ co-treatment, $P = 0.019$). The treatment of CsA alone was without significant effect on MitoSox Red intensity (Fig. 2B. CsA-treatment vs. control. $P > 0.05$). These data suggest that the blockage of CypD by genetic depletion or pharmacological inhibition suppresses Aβ-induced increase in mitochondrial ROS production/accumulation.

To determine the involvement of CypD in Aβ-instigated PKA/CREB signaling transduction change, we next evaluated alterations in PKA activity in Aβ-treated cultured neurons in the presence (nonTg) and absence (CypD-deficient, *Ppif*$^{-/-}$) of CypD. Aβ treatment caused a time-dependent decrease in PKA activity in nonTg neurons compared to the vehicle treatment (Fig. 3A, Aβ 2 h: 0.76 ± 0.047, Aβ 6 h: 0.72 ± 0.032, Aβ 12 h: 0.61 ± 0.057, Aβ 24 h: 0.59 ± 0.037 vs. vehicle:1 ± 0.056). In contrast, PKA activity in *Ppif*$^{-/-}$ neurons remained constant over the entire period of Aβ-treatment for 2 to 24 hours; and Aβ-insulted nonTg neurons demonstrated significantly suppressed PKA activity in comparison to their corresponding Aβ-treated *Ppif*$^{-/-}$ neurons. Utilization of KT5720, a selective inhibitor of PKA activity that acts as an antagonist at the PKA-ATP binding site of the PKA C, efficiently inhibited PKA activity in both types of neurons (Fig. 3A). These results indicate that lack of CypD rescues Aβ-induced inactivation of PKA.

Then, we examined the phosphorylation of the PKA C Thr197 (p-PKA C) in Aβ superimposed neurons. Aβ-treated nonTg neurons had a 45% decrease in p-PKAc compared to the vehicle control (Fig. 3B). No changes of p-PKA C were observed in *Ppif*$^{-/-}$ neurons (Fig. 3B). The close correlation of decrease in p-PKA C to reduced PKA activity indicates that Aβ-induced dephosphorylation of PKA C is responsible for inhibiting PKA activity, and that CypD deficiency attenuates Aβ-induced inhibitory effect on PKA activation.

At last, we examined the effect of CypD deficiency on Aβ-induced CREB phosphorylation. In the presence of Aβ, glutamate-induced pCREB was significantly reduced in nonTg neurons as compared with the vehicle control (Fig. 3C); while the pCREB level was substantially preserved in Aβ-insulted CypD-deficient neurons (Fig. 3C). The addition of rolipram (3 μM) or forskolin (5 μM) that activates PKA reversed Aβ-induced depression of pCREB (Fig. 3C), indicating that the PKA activation is critical for enhancing CREB activity against Aβ toxicity. It is noted that the expression levels of total CREB remained no significant changes among indicated groups of cells. These studies indicate that CypD abrogation protects against Aβ-induced down-regulation of the PKA signaling cascade.

3.3. CypD deficiency rescues Aβ-induced loss of synapses associated with PKA/CREB signaling transduction pathway preservation

PKA/CREB signaling transduction pathway plays an essential role in controlling and regulating synaptic plasticity. To address whether CypD-deficiency protected PKA/CREB signal transduction pathway connects to synaptic damage in Aβ-insulted neurons, we analyzed the effect of CypD depletion on Aβ-induced synaptic loss. Synapses were identified as synaptophysin-positive clusters attaching to dendrites. The recruitment of the presynaptic protein, synaptophysin to form synaptophysin-positive clusters is synaptic activity dependent and in a rapid manner [41]. Synaptophysin expression level in Aβ treated nonTg and *Ppif*$^{-/-}$ neurons were detected by Western blot. The level of synaptophysin expression was significantly reduced by 50% in Aβ-treated nonTg neurons compared to the vehicle treated groups (Fig. 4A). CypD deficiency largely reversed Aβ-induced decrease in synaptophysin expression (14% decrease in *Ppif*$^{-/-}$ neurons compared to nonTg neurons in the presence of Aβ). Synaptic density was quantified as the number of synaptophysin positive clusters per micron of dendrite length. After Aβ treatment, synaptic density in nonTg neurons was decreased by 41% in comparison to those in vehicle-treated controls (Fig. 4B, Aβ: 0.415 ± 0.024 versus vehicle: 0.647 ± 0.021); while CypD deficiency largely reversed Aβ-induced decrease in synaptic density (Fig. 4B, *Ppif*$^{-/-}$: 0.510 ± 0.018 versus nonTg: 0.415 ± 0.024). Forskolin, PKA activator, protected against Aβ-induced synaptic density loss (Fig. 4B, Forskolin: 0.656 ± 0.022 versus Aβ: 0.415 ± 0.024), indicating that Aβ-induced loss of synapses associated with PKA/CREB signaling transduction pathway. CypD-deficiency also largely reversed Aβ-induced decrease in postsynaptic GluR1 cluster (S1).

In furtherance, antioxidant probucol or pharmacological scavengers of ROS (SOD/catalase) were added to neurons in culture to determine the effect of oxidative stress. As shown in Fig. 4C, antioxidants remarkably reversed Aβ-induced synaptic loss. In the presence of Aβ, nonTg neurons demonstrated a decrease of 34.2% in synaptic density in comparison to the vehicle control (Fig. 4C), while SOD/catalase and probucol significantly increased synaptic density by 30–35% (Fig. 4C; SOD/catalase + Aβ: 0.538 ± 0.027, probucol + Aβ: 0.559 ± 0.023). Neither SOD/catalase nor probucol alone interfered with synaptophysin cluster density in neurons (Fig. 4C). The results of in vitro synaptic density experiments suggest that either CypD depletion or elimination of ROS by antioxidants protects synapses against Aβ insults, which is in accordance with preserved PKA/CREB signaling transduction pathway in an environment enriched for Aβ.

3.4. CypD deficiency suppresses oxidative stress in mAPP mice

As aforementioned, our results showed that Aβ-impaired PKA/CREB signaling transduction cascade is closely correlated with CypD-associated oxidative stress in vitro neuronal culture. Next, we extended our observation on the protective effect of CypD deficiency in an in vitro cultured neurons to an in vivo AD mouse model overexpressing Aβ (mAPP mice) that resembles Aβ pathology in human AD brain. Brain cortexes derived from 12-month old mAPP mice, age-matched nonTg, CypD deficient, and CypD-deficient mAPP mice were subjected to the assay of oxidative stress marker 4-HNE (4-Hydroxynonenal). mAPP mice demonstrated significantly higher levels of 4-HNE than nonTg littermates (Fig. 5A; $P = 0.0267$). In contrast, the 4-HNE level was significantly reduced in CypD-deficient mAPP mice (Fig. 5A; mAPP mice vs. mAPP/*Ppif*$^{-/-}$ mice, $P = 0.0321$). CypD deficient mice did not show significant difference in 4-HNE level as compared to nonTg mice (Fig. 5A; $P > 0.05$). These results are consistent with our previous study showing that CypD-deficient mAPP mice had less mitochondrial ROS level than mAPP mice at the age of 12 months [19]. In combination, our results suggest that CypD deficiency protects brains from oxidative stress in mAPP mice, which is correlated to our in vitro results on the protective effect of CypD depletion on Aβ-induced ROS production.

3.5. CypD deficiency protects PKA/CREB signaling transduction pathway in mAPP mice

In view of the protective effects of CypD deficiency on Aβ-impaired PKA/CREB signaling transduction pathway and the subsequent synaptic change in anin vitro neuronal culture model, we examined the involvement of CypD-related perturbation in PKA/CREB pathway in mAPP mice. We first measured PKA activity in brain extracts of Tg mice including nonTg, APP/Aβ overexpression (mAPP), CypD deficient (*Ppif*$^{-/-}$) and CypD-deficient mAPP (mAPP/*Ppif*$^{-/-}$) mice at 12-month-old. Consistent with the effect of Aβ on in vitro cultured neurons, PKA activity was significantly lowered in mAPP mice than in nonTg littermate controls, while PKA activity in mAPP/*Ppif*$^{-/-}$ mice was effectively restored (Fig. 5B). Accordingly, p-PKA C levels were significantly suppressed in mAPP mice but not in mAPP/*Ppif*$^{-/-}$, nonTg and *Ppif*$^{-/-}$ mice (Fig. 5C).

Next, we measured levels of phosphorylation of CREB ser133 (pCREB) in cortex extracts by ELISA. The levels of pCREB were significantly reduced in mAPP mice as compared with nonTg mice (30% decreased over nonTg mice), whereas mAPP/*Ppif*$^{-/-}$ mice had higher levels of pCREB than mAPP mice (Fig. 5D). The levels of pCREB in nonTg mice were comparable to *Ppif*$^{-/-}$ mice. Total CREB levels were not changed among all the groups of mice. These observations indicate that abrogation of CypD rescues PKA/CREB signaling trans-duction pathway in mAPP mice.

3.6. Lack of CypD improves synaptic activity/transmission and alleviates deficits in dendritic spine architecture in mAPP mice

To determine the involvement of CypD in synaptic activity, we analyzed changes in Spontaneous Miniature Excitatory Postsynaptic Currents (mEPSCs) in CA1 neurons in brain slices from 12-month-old mAPP mice compared to those from nonTg, *Ppif*$^{-/-}$ and mAPP/*Ppif*$^{-/-}$ mice. The amplitude of mEPSCs in mAPP neurons was significantly decreased by 24% as compared to those in nonTg neurons (Fig. 6A, mAPP: 10.08 ± 0.28 versus nonTg:

13.28 ± 0.79). Similarly, the mEPSC frequency in mAPP neurons was substantially reduced by 38.5% (Fig. 6B, mAPP: 0.24 ± 0.046 versus nonTg: 0.39 ± 0.44). Importantly, CypD deficiency significantly restored mEPSC amplitude and frequency in mAPP/*Ppif*$^{-/-}$ neurons (Fig. 6A–B, amplitude: 11.45 ± 0.47, frequency: 0.39 ± 0.044).

We next studied whether the impairments in synaptic activity were linked to the loss of dendritic spines and changes in spine morphology. Since the basal dendrites of CA1 neurons receive input from CA3 neurons through Schaffer collaterals and are thought to be an infrastructure basis of the consolidation of long term potentiation [42], we analyzed basal dendritic spine architecture in the hippocampal CA1 neurons of Tg mice. We measured spine density and found that mAPP CA1 neurons had 20% less spine density than nonTg CA1 neurons (Fig. 7A1, 0.83 ± 0.088 versus 1.03 ± 0.032 per micron), whereas mAPP/*Ppif*$^{-/-}$ CA1 neurons showed a smaller decrease (∼4%) in dendritic spine density (Fig. 7A1, 0.97 ± 0.035 versus 1.03 ± 0.032 per micron). Cumulative percentile curves of spine density displayed an apparent left shift in mAPP neurons compared to those of nonTg, *Ppif*$^{-/-}$ and mAPP/*Ppif*$^{-/-}$ neurons (Fig. 7A2). These results demonstrate the protective effect of CypD depletion on the dendritic spine loss in mAPP mice.

We then evaluated the effect of CypD on dendritic spine morphology by intra-neuronal injection of Lucifer yellow (Fig. 7E, S2-3) and categorized dendritic spins into three groups (mushroom, stubby and thin) [36,43]. Results of quantitative analysis of basal dendritic spines in nonTg CA1 neurons showed 43.2%, 12.3%, and 44.6% for mushroom, stubby, and thin spines, respectively. Interestingly, mAPP CA1 neurons showed a significantly decreased percentage of mushroom spines (Fig. 7B1–2, mAPP: 24.31 ± 1.02 versus nonTg: 43.18 ± 1.72), but an increased percentage of stubby spines (Fig. 7C1–2, mAPP: 25.47 ± 1.36 versus nonTg: 12.25 ± 0.83). Besides there was a 10% increase in thin spines in mAPP neurons (Fig. 7D1–2, mAPP: 50.22 ± 1.11 versus nonTg: 45.20 ± 1.70), suggesting that dendritic spine maturation is altered in mAPP mice. Remarkably, CypD-deficient mAPP neurons significantly preserved dendritic spine morphology as shown by an increased percentage of mushroom spines (Fig. 7B1, 35.26 ± 1.1) and reduced percentage of stubby spines (Fig. 7C1, 17.04 ± 1.19). Plots of cumulative percentage curves for the different types of dendritic spines clearly showed a substantial left shift of the curve for mushroom spines and a right shift for stubby spines in mAPP CA1 neurons, while the indicated curves of mushroom or stubby spines of mAPP/*Ppif*$^{-/-}$ neurons fell between those of mAPP and nonTg neurons (Fig. 7B2 and C2). Notably, CypD deficient neurons demonstrated increased percentage of thin spines comparing to nonTg neurons, while there is no significant difference in the percentage of mushroom and stubby spines between nonTg and CypD deficient neurons suggesting the dendritic spine development in *Ppif*$^{-/-}$ neurons is more active. Taken together, these data indicate that CypD depletion significantly preserves dendritic spine maturation and morphology with improved synaptic activity, and ultimately attenuated synaptic degeneration in mAPP mice.

4. Discussion

The synchronization of mitochondrial pathology and synaptic alterations in AD has been previously acknowledged, but the mechanism underlying the interplay of neuronal

mitochondrial dysfunction and synaptic change in AD remains largely unknown. This study was the first report that CypD mediates PKA signaling perturbation contributes to Aβ-induced synaptic damages including alterations in synaptic structure and synaptic function. First, we showed that CypD-deficiency attenuated Aβ-mediated reduction in PKA activity and phosphorylation of PKA C and CREB. Second, antioxidant probucol or SOD/catalase, pharmacological scavengers of ROS blunted Aβ-induced inactivation of PKA/CREB signaling. Third, neurons lacking CypD were resistant to Aβ-induced loss of synapses. Finally, these protective effects of CypD deficiency on disruption of signal transduction and deficits in synaptic structure and function were observed in CypD-deficient mAPP mice in contrast with mAPP mice. Our results indicate that CypD-mediated increase in mitochondrial and intracellular oxidative stress inhibits PKA catalytic subunit phosphorylation and subsequently disrupts the PKA/CREB signaling transduction pathway, eventually leading to structural and functional synaptic deterioration. Notably, abrogation of CypD restores PKA/CREB signaling and attenuates further synaptic aberrations. In conclusion, CypD-mediated PKA/CREB signal transduction disruption appears to be an important player in the scenario leading to synaptic injury in Aβ milieu (Fig. 8).

Oxidative stress is culprit for many intracellular perturbations like protein misfolding and inactivation, nucleic and mitochondrial DNA injuries [44–46]. Increasing evidence has shown that oxidative stress alters PKA activity and phosphorylation of CREB, which is detrimental to cell survival [47,48]. Indeed, we demonstrated that the phosphorylation of PKA C subunit at Thr197 is susceptible to the insult of pro-oxidant (t-butyl hydroperoxide, TBH) (S4). Aβ is a strong instigator of both extracellular and intracellular ROS production leading to intra-cellular oxidative stress and protein oxidation in AD brains. In this study, we employed SOD/catalase to scavenge extracellular and intra-cellular oxidative stress aroused by Aβ, respectively. Given that probucol is an antioxidant preventing protein or lipid peroxidation and that the addition of probucol attenuates oxidative stress [38,39], we also chose probucol as an antioxidant for this study. Consistent with the results from SOD/catalase, ROS scavengers, probucol treatment significantly blocked inhibitory effects of Aβ on phosphorylation of PKA C, PKA activity, pCREB (Fig. 1), and density of synapses (Fig. 4).

The application of antioxidants significantly protects neurons from Aβ-induced inactivation of PKA, suggesting that Aβ-associated oxidative stress underlies perturbed PKA/CREB signaling transduction in AD. In fact, the treatment of Aβ also has effect on inducing mitochondrial ROS overproduction. We propose that Aβ induces the formation of mPTP, which is a severe mitochondrial pathology in AD, resulting in mitochondrial ROS overproduction and release to cytosol to break cytosolic Redox balance [19]. In correlation with previous reports that the depletion of CypD significantly diminishes mitochondrial ROS generation and suppresses the subsequent cytosolic ROS elevation, our results demonstrate that CypD deficiency is closely associated with preserved PKA activity and the downstream CREB signaling cascade from Aβ toxicity. Aβ-induced mitochondrial ROS perturbation through CypD-mediated mPTP contributes to PKA/CREB disturbances in AD. It is noted that increased intracellular ROS is an inductive factor of CypD-mediated mPTP formation, which in turn results in mitochondrial ROS overproduction and release, and eventually exaggerated intracellular oxidative stress. The feed-back loop of intracellular oxidative

stress and mPTP-associated ROS has been well documented. Several previous studies have demonstrated that the application of antioxidants including exogenous SOD/catalase to prevent oxidizing reagent-induced extra- and intra-cellular oxidative stress is effective in blunting mPTP formation and thusly reducing ROS-associated oxidative stress in cells [49,50]. It therefore serves as indicative evidence that the antioxidants we adopted in this study attenuated Aβ-suppressed PKA/CREB activity at least partially through the inhibition of CypD-mediated mPTP formation. Indeed, CypD-associated cytosolic ROS elevation is closely related to the formation of mPTP, which is a mechanism of mitochondria-generated ROS release. The application of mitochondria-targeted antioxidants might be another option to extinguish the mPTP-associated mitochondrial ROS production and further protect PKA signaling cascades from Aβ toxicity. In fact, several studies have suggested that the application of mitochondria-targeted antioxidants significantly attenuated CypD-associated cell perturbations [51,52]. However, recent studies showed that the application of mitochondria-targeted antioxidants such as MitoQ and Resveratrol substantially decreased the expression level of CypD in primary cultured hippocampal neurons, suggesting the modulating effect of mitochondria-targeted antioxidants on CypD transcription and expression [51]. In view of the purpose of the current study to reveal the mechanisms underlying CypD-mediated mPTP and cytosolic PKA activity disturbances, we chose antioxidants only targeted to intracellular and extracellular ROS without interfering the baseline expression levels of CypD under our experimental conditions (data not shown). The dual effects of mitochondria-targeted antioxidants that diminish mitochondrial ROS and down-regulate CypD expression levels suggest that mitochondria-targeted antioxidant is a promising strategy against CypD-associated neuronal stresses. We will perform a detailed study to evaluate the effect of mitochondria-targeted antioxidants as a treatment strategy for AD in our future work.

Intracellular oxidative stress and calcium elevation are two major consequences of CypD-mediated mPTP formation. We have shown that increased intracellular ROS significantly inhibits PKA activity. We then tested the effects of elevated intracellular calcium on PKA by using A23187 (calcium ionophore). Administration of A23187 to nonTg neurons did not change PKA C phosphorylation (data not shown), suggesting PKA C phosphorylation is not sensitive to intracellular calcium elevation. In view of our data showing the protective effects of antioxidants (SOD/catalase, and probucol) and CypD blockade on Aβ-impaired PKA/CREB signal, CypD-associated oxidative stress is likely to be a major player for Aβ-induced suppression of PKA activity.

The PKA/CREB signaling cascade plays a crucial role in regulation of neuronal/synaptic function, such as synaptic maturation and long-term memory consolidation. PKA untethers synaptic vesicles, regulates the functions of NMDA (N-methyl-D-aspirate receptor) and AMPA (α-amino-3-hydroxy-5-methyl-4-isoxazole propionate receptor) receptors and phosphorylates several synapse-related proteins (i.e., PSD95, snapin and synapsin), suggesting that PKA is critical for synaptic transmission, dendritic spine architecture and synaptic maturation [26,31,53–55]. Notably, PKA function depends on the activation of PKA C and activation of PKA C relies on phosphorylation at the proper sites, Thr197. Phosphorylation at Thr197 site stabilizes PKA C structure, exposes its activation site, and facilitates its binding to PKA regulatory subunit [56,57]. Our study provides evidence of the

negative effect of CypD-associated oxidative stress on PKA C Thr197 phos-phorylation, PKA activity and CREB phosphorylation, leading to a compromised PKA/CREB signaling cascade; and as a contrast, genetic depletion of CypD significantly blocked Aβ-induced PKA deactivation. Furthermore, application of CypD inhibitor has a protection against Aβ-induced PKA perturbations. It is possible that CypD/Aβ-dependent synaptic dysfunction may also involve other mechanisms such as decreased synaptic mitochondrial energy production and disturbed Ca^{2+}-regulated signaling pathways including calmodulin-dependent protein kinase II (CaMKII), calcineurin and/or Protein Kinase C (PKC) in addition to PKA/CREB pathway [34,40,58–60]. These CypD-related changes are potential mechanisms in addition to deactivation of PKA/CREB pathway, contributing to synaptic degeneration in AD; hereby, further investigations are also required for elucidating these alternative mechanisms.

In view of the involvement of CypD in Aβ-mediated oxidative stress and PKA/CREB signaling transduction pathway perturbation, we propose that sustained CypD-induced neuronal/synaptic mitochondrial stress is a potential mechanism responsible for synaptic failure in the pathogenesis of AD. Our postulation is based on our finding that mAPP mice revealed abnormalities in dendritic spine architecture, dendritic spine maturation, and spontaneous synaptic activity. These synaptic alterations were substantially reversed in CypD-depleted mAPP mice. Together with the protection of CypD ablation on Aβ-induced impairments in hippocampal long-term potentiation (LTP) and learning/memory ability [19,25], our studies gain new insights into the role of CypD-dependent mitochondrial ROS in disturbing synaptic plasticity and maturation in AD. Hence, blockade of CypD may be potential therapeutic strategy for preventing and halting synaptic and mitochondrial pathology in Alzheimer disease.

Supplementary Material

Refer to Web version on PubMed Central for supplementary material.

Acknowledgments

This study is supported by grants from the National Institute of Aging (R37AG037319, PO1AG017490, and K99AG037716), and the National Institute of General Medical Science (R01GM095355).

References

1. von Gunten A, Kovari E, Bussiere T, Rivara CB, Gold G, Bouras C, Hof PR, Giannakopoulos P. Cognitive impact of neuronal pathology in the entorhinal cortex and CA1 field in Alzheimer's disease. Neurobiol Aging. 2006; 27:270–277. [PubMed: 16399212]
2. Cummings BJ, Pike CJ, Shankle R, Cotman CW. Beta-amyloid deposition and other measures of neuropathology predict cognitive status in Alzheimer's disease. Neurobiol Aging. 1996; 17:921–933. [PubMed: 9363804]
3. Scheff SW, Price DA, Schmitt FA, Mufson EJ. Hippocampal synaptic loss in early Alzheimer's disease and mild cognitive impairment. Neurobiol Aging. 2006; 27:1372–1384. [PubMed: 16289476]
4. Selkoe DJ. Alzheimer's disease is a synaptic failure. Science. 2002; 298:789–791. [PubMed: 12399581]

5. Yao J, Irwin RW, Zhao L, Nilsen J, Hamilton RT, Brinton RD. Mitochondrial bio-energetic deficit precedes Alzheimer's pathology in female mouse model of Alzheimer's disease. Proc Natl Acad Sci U S A. 2009; 106:14670–14675. [PubMed: 19667196]

6. Takuma K, Yao J, Huang J, Xu H, Chen X, Luddy J, Trillat AC, Stern DM, Arancio O, Yan SS. ABAD enhances Abeta-induced cell stress via mitochondrial dysfunction. FASEB J. 2005; 19:597–598. [PubMed: 15665036]

7. Caspersen C, Wang N, Yao J, Sosunov A, Chen X, Lustbader JW, Xu HW, Stern D, McKhann G, Yan SD. Mitochondrial Abeta: a potential focal point for neuronal metabolic dysfunction in Alzheimer's disease. FASEB J. 2005; 19:2040–2041. [PubMed: 16210396]

8. Manczak M, Anekonda TS, Henson E, Park BS, Quinn J, Reddy PH. Mitochondria are a direct site of A beta accumulation in Alzheimer's disease neurons: implications for free radical generation and oxidative damage in disease progression. Hum Mol Genet. 2006; 15:1437–1449. [PubMed: 16551656]

9. Lin MT, Beal MF. Alzheimer's APP mangles mitochondria. Nat Med. 2006; 12:1241–1243. [PubMed: 17088888]

10. Eckert A, Hauptmann S, Scherping I, Rhein V, Muller-Spahn F, Gotz J, Muller WE. Soluble beta-amyloid leads to mitochondrial defects in amyloid precursor protein and tau transgenic mice. Neurodegener Dis. 2008; 5:157–159. [PubMed: 18322377]

11. Lustbader JW, Cirilli M, Lin C, Xu HW, Takuma K, Wang N, Caspersen C, Chen X, Pollak S, Chaney M, Trinchese F, Liu S, Gunn-Moore F, Lue LF, Walker DG, Kuppusamy P, Zewier ZL, Arancio O, Stern D, Yan SS, Wu H. ABAD directly links Abeta to mitochondrial toxicity in Alzheimer's disease. Science. 2004; 304:448–452. [PubMed: 15087549]

12. Cardoso SM, Santana I, Swerdlow RH, Oliveira CR. Mitochondria dysfunction of Alzheimer's disease cybrids enhances Abeta toxicity. J Neurochem. 2004; 89:1417–1426. [PubMed: 15189344]

13. Hensley K, Carney JM, Mattson MP, Aksenova M, Harris M, Wu JF, Floyd RA, Butterfield DA. A model for beta-amyloid aggregation and neurotoxicity based on free radical generation by the peptide: relevance to Alzheimer disease. Proc Natl Acad Sci U S A. 1994; 91:3270–3274. [PubMed: 8159737]

14. Chang DT, Honick AS, Reynolds IJ. Mitochondrial trafficking to synapses in cultured primary cortical neurons. J Neurosci. 2006; 26:7035–7045. [PubMed: 16807333]

15. Wang X, Su B, Siedlak SL, Moreira PI, Fujioka H, Wang Y, Casadesus G, Zhu X. Amyloid-beta overproduction causes abnormal mitochondrial dynamics via differential modulation of mitochondrial fission/fusion proteins. Proc Natl Acad Sci U S A. 2008; 105:19318–19323. [PubMed: 19050078]

16. Calkins MJ, Reddy PH. Amyloid beta impairs mitochondrial anterograde transport and degenerates synapses in Alzheimer's disease neurons. Biochim Biophys Acta. 2011; 1812:507–513. [PubMed: 21241801]

17. Calkins MJ, Manczak M, Mao P, Shirendeb U, Reddy PH. Impaired mitochondrial biogenesis, defective axonal transport of mitochondria, abnormal mitochondrial dynamics and synaptic degeneration in a mouse model of Alzheimer's disease. Hum Mol Genet. 2011; 20:4515–4529. [PubMed: 21873260]

18. Manczak M, Reddy PH. Abnormal interaction of VDAC1 with amyloid beta and phosphorylated tau causes mitochondrial dysfunction in Alzheimer's disease. Hum Mol Genet. 2012; 21:5131–5146. [PubMed: 22926141]

19. Du H, Guo L, Fang F, Chen D, Sosunov AA, McKhann GM, Yan Y, Wang C, Zhang H, Molkentin JD, Gunn-Moore FJ, Vonsattel JP, Arancio O, Chen JX, Yan SD. Cyclophilin D deficiency attenuates mitochondrial and neuronal perturbation and ameliorates learning and memory in Alzheimer's disease. Nat Med. 2008; 14:1097–1105. [PubMed: 18806802]

20. Moreira PI, Santos MS, Moreno A, Rego AC, Oliveira C. Effect of amyloid beta-peptide on permeability transition pore: a comparative study. J Neurosci Res. 2002; 69:257–267. [PubMed: 12111807]

21. Hansson Petersen CA, Alikhani N, Behbahani H, Wiehager B, Pavlov PF, Alafuzoff I, Leinonen V, Ito A, Winblad B, Glaser E, Ankarcrona M. The amyloid beta-peptide is imported into

mitochondria via the TOM import machinery and localized to mitochon-drial cristae. Proc Natl Acad Sci U S A. 2008; 105:13145–13150. [PubMed: 18757748]

22. Crouch PJ, Blake R, Duce JA, Ciccotosto GD, Li QX, Barnham KJ, Curtain CC, Cherny RA, Cappai R, Dyrks T, Masters CL, Trounce IA. Copper-dependent inhibition of human cytochrome c oxidase by a dimeric conformer of amyloid-beta1–42. J Neurosci. 2005; 25:672–679. [PubMed: 15659604]
23. Du H, Guo L, Yan S, Sosunov AA, McKhann GM, Yan SS. Early deficits in synaptic mitochondria in an Alzheimer's disease mouse model. Proc Natl Acad Sci U S A. 2010; 107:18670–18675. [PubMed: 20937894]
24. Manczak M, Calkins MJ, Reddy PH. Impaired mitochondrial dynamics and abnormal interaction of amyloid beta with mitochondrial protein Drp1 in neurons from patients with Alzheimer's disease: implications for neuronal damage. Hum Mol Genet. 2011; 20:2495–2509. [PubMed: 21459773]
25. Du H, Guo L, Zhang W, Rydzewska M, Yan S. Cyclophilin D deficiency improves mitochondrial function and learning/memory in aging Alzheimer disease mouse model. Neurobiol Aging. 2011; 32:398–406. [PubMed: 19362755]
26. Gong B, Cao Z, Zheng P, Vitolo OV, Liu S, Staniszewski A, Moolman D, Zhang H, Shelanski M, Arancio O. Ubiquitin hydrolase Uch-L1 rescues beta-amyloid-induced decreases in synaptic function and contextual memory. Cell. 2006; 126:775–788. [PubMed: 16923396]
27. Nguyen PV, Woo NH. Regulation of hippocampal synaptic plasticity by cyclic AMP-dependent protein kinases. Prog Neurobiol. 2003; 71:401–437. [PubMed: 15013227]
28. Lonart G, Schoch S, Kaeser PS, Larkin CJ, Sudhof TC, Linden DJ. Phosphorylation of RIM1alpha by PKA triggers presynaptic long-term potentiation at cerebellar parallel fiber synapses. Cell. 2003; 115:49–60. [PubMed: 14532002]
29. Powell CM. Gene targeting of presynaptic proteins in synaptic plasticity and memory: across the great divide. Neurobiol Learn Mem. 2006; 85:2–15. [PubMed: 16230036]
30. Zheng Z, Keifer J. PKA has a critical role in synaptic delivery of GluR1- and GluR4-containing AMPARs during initial stages of acquisition of in vitro classical conditioning. J Neurophysiol. 2009; 101:2539–2549. [PubMed: 19261706]
31. Esteban JA, Shi SH, Wilson C, Nuriya M, Huganir RL, Malinow R. PKA phosphorylation of AMPA receptor subunits controls synaptic trafficking underlying plasticity. Nat Neurosci. 2003; 6:136–143. [PubMed: 12536214]
32. Smith DL, Pozueta J, Gong B, Arancio O, Shelanski M. Reversal of long-term dendritic spine alterations in Alzheimer disease models. Proc Natl Acad Sci U S A. 2009; 106:16877–16882. [PubMed: 19805389]
33. Mucke L, Masliah E, Yu GQ, Mallory M, Rockenstein EM, Tatsuno G, Hu K, Kholodenko D, Johnson-Wood K, McConlogue L. High-level neuronal expression of abeta 1–42 in wild-type human amyloid protein precursor transgenic mice: synaptotoxicity without plaque formation. J Neurosci. 2000; 20:4050–4058. [PubMed: 10818140]
34. Origlia N, Righi M, Capsoni S, Cattaneo A, Fang F, Stern DM, Chen JX, Schmidt AM, Arancio O, Yan SD, Domenici L. Receptor for advanced glycation end product-dependent activation of p38 mitogen-activated protein kinase contributes to amyloid-beta-mediated cortical synaptic dysfunction. J Neurosci. 2008; 28:3521–3530. [PubMed: 18367618]
35. Hyde BB, Liesa M, Elorza AA, Qiu W, Haigh SE, Richey L, Mikkola HK, Schlaeger TM, Shirihai OS. The mitochondrial transporter ABC-me (ABCB10), a downstream target of GATA-1, is essential for erythropoiesis in vivo. Cell Death Differ. 2012; 19:1117–1126. [PubMed: 22240895]
36. Harris KM, Jensen FE, Tsao B. Three-dimensional structure of dendritic spines and synapses in rat hippocampus (CA1) at postnatal day 15 and adult ages: implications for the maturation of synaptic physiology and long-term potentiation. J Neurosci Off J Soc Neurosci. 1992; 12:2685–2705.
37. Humphries KM, Deal MS, Taylor SS. Enhanced dephosphorylation of cAMP-dependent protein kinase by oxidation and thiol modification. J Biol Chem. 2005; 280:2750–2758. [PubMed: 15533936]

38. Yan SD, Schmidt AM, Anderson GM, Zhang J, Brett J, Zou YS, Pinsky D, Stern D. Enhanced cellular oxidant stress by the interaction of advanced glycation end products with their receptors/binding proteins. J Biol Chem. 1994; 269:9889–9897. [PubMed: 8144582]

39. Guo L, Du H, Yan S, Wu X, McKhann GM, Chen JX, Yan SS. Cyclophilin d deficiency rescues axonal mitochondrial transport in Alzheimer's neurons. PLoS One. 2013; 8:e54914. [PubMed: 23382999]

40. Vitolo OV, Sant'Angelo A, Costanzo V, Battaglia F, Arancio O, Shelanski M. Amyloid beta-peptide inhibition of the PKA/CREB pathway and long-term potentiation: reversibility by drugs that enhance cAMP signaling. Proc Natl Acad Sci U S A. 2002; 99:13217–13221. [PubMed: 12244210]

41. Jin I, Udo H, Hawkins RD. Rapid increase in clusters of synaptophysin at onset of homosynaptic potentiation in Aplysia. Proc Natl Acad Sci U S A. 2011; 108:11656–11661. [PubMed: 21709228]

42. Kaibara T, Leung LS. Basal versus apical dendritic long-term potentiation of commissural afferents to hippocampal CA1: a current-source density study. J Neurosci. 1993; 13:2391–2404. [PubMed: 8501513]

43. Yuste R, Bonhoeffer T. Morphological changes in dendritic spines associated with long-term synaptic plasticity. Annu Rev Neurosci. 2001; 24:1071–1089. [PubMed: 11520928]

44. Barrett MJ, Alones V, Wang KX, Phan L, Swerdlow RH. Mitochondria-derived oxidative stress induces a heat shock protein response. J Neurosci Res. 2004; 78:420–429. [PubMed: 15389841]

45. Jacobson J, Duchen MR. Mitochondrial oxidative stress and cell death in astrocytes–requirement for stored Ca2+ and sustained opening of the permeability transition pore. J Cell Sci. 2002; 115:1175–1188. [PubMed: 11884517]

46. Naoi M, Maruyama W, Shamoto-Nagai M, Yi H, Akao Y, Tanaka M. Oxidative stress in mitochondria: decision to survival and death of neurons in neurodegenerative disorders. Mol Neurobiol. 2005; 31:81–93. [PubMed: 15953813]

47. Chiueh CC, Andoh T, Chock PB. Induction of thioredoxin and mitochondrial survival proteins mediates preconditioning-induced cardioprotection and neuroprotection. Ann N Y Acad Sci. 2005; 1042:403–418. [PubMed: 15965087]

48. Valera E, Sanchez-Martin FJ, Ferrer-Montiel AV, Messeguer A, Merino JM. NMDA-induced neuroprotection in hippocampal neurons is mediated through the protein kinase A and CREB (cAMP-response element-binding protein) pathway. Neurochem Int. 2008; 53:148–154. [PubMed: 18694792]

49. Valle VG, Fagian MM, Parentoni LS, Meinicke AR, Vercesi AE. The participation of reactive oxygen species and protein thiols in the mechanism of mitochondrial inner membrane permeabilization by calcium plus prooxidants. Arch Biochem Biophys. 1993; 307:1–7. [PubMed: 8239645]

50. Vercesi AE, Kowaltowski AJ, Grijalba MT, Meinicke AR, Castilho RF. The role of reactive oxygen species in mitochondrial permeability transition. Biosci Rep. 1997; 17:43–52. [PubMed: 9171920]

51. Manczak M, Mao P, Calkins MJ, Cornea A, Reddy AP, Murphy MP, Szeto HH, Park B, Reddy PH. Mitochondria-targeted antioxidants protect against amyloid-beta toxicity in Alzheimer's disease neurons. J Alzheimers Dis. 2010; 20(Suppl. 2):S609–S631. [PubMed: 20463406]

52. Lopez-Erauskin J, Galino J, Bianchi P, Fourcade S, Andreu AL, Ferrer I, Munoz-Pinedo C, Pujol A. Oxidative stress modulates mitochondrial failure and cyclophilin D function in X-linked adrenoleukodystrophy. Brain. 2012; 135:3584–3598. [PubMed: 23250880]

53. Chetkovich DM, Chen L, Stocker TJ, Nicoll RA, Bredt DS. Phosphorylation of the postsynaptic density-95 (PSD-95)/discs large/zona occludens-1 binding site of stargazin regulates binding to PSD-95 and synaptic targeting of AMPA receptors. J Neurosci. 2002; 22:5791–5796. [PubMed: 12122038]

54. Skeberdis VA, Chevaleyre V, Lau CG, Goldberg JH, Pettit DL, Suadicani SO, Lin Y, Bennett MV, Yuste R, Castillo PE, Zukin RS. Protein kinase A regulates calcium permeability of NMDA receptors. Nat Neurosci. 2006; 9:501–510. [PubMed: 16531999]

55. Kuromi H, Kidokoro Y. Exocytosis and endocytosis of synaptic vesicles and functional roles of vesicle pools: lessons from the *Drosophila* neuromuscular junction. Neuroscientist. 2005; 11:138–147. [PubMed: 15746382]

56. Yonemoto W, Garrod SM, Bell SM, Taylor SS. Identification of phosphorylation sites in the recombinant catalytic subunit of cAMP-dependent protein kinase. J Biol Chem. 1993; 268:18626–18632. [PubMed: 8395513]

57. Iyer GH, Moore MJ, Taylor SS. Consequences of lysine 72 mutation on the phosphorylation and activation state of cAMP-dependent kinase. J Biol Chem. 2005; 280:8800–8807. [PubMed: 15618230]

58. Arancio O, Zhang HP, Chen X, Lin C, Trinchese F, Puzzo D, Liu S, Hegde A, Yan SF, Stern A, Luddy JS, Lue LF, Walker DG, Roher A, Buttini M, Mucke L, Li W, Schmidt AM, Kindy M, Hyslop PA, Stern DM, Du Yan SS. RAGE potentiates Abeta-induced perturbation of neuronal function in transgenic mice. EMBO J. 2004; 23:4096–4105. [PubMed: 15457210]

59. Yan SD, Chen X, Fu J, Chen M, Zhu H, Roher A, Slattery T, Zhao L, Nagashima M, Morser J, Migheli A, Nawroth P, Stern D, Schmidt AM. RAGE and amyloid-beta peptide neurotoxicity in Alzheimer's disease. Nature. 1996; 382:685–691. [PubMed: 8751438]

60. Xie Y, Deng S, Chen Z, Yan S, Landry DW. Identification of small-molecule inhibitors of the Abeta–ABAD interaction. Bioorg Med Chem Lett. 2006; 16:4657–4660. [PubMed: 16781151]

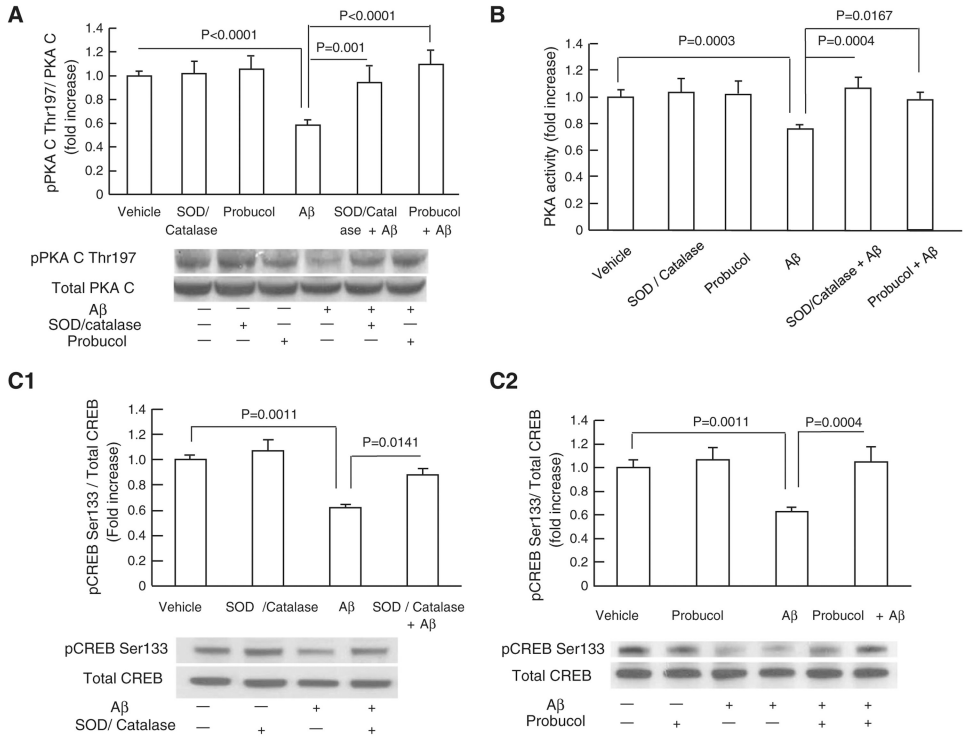

Fig. 1.

Antioxidants attenuated Aβ-induced inhibitory effects on pPKA C and pCREB levels. (A) The treatment of SOD (200 U/ml)/catalase (250 U/ml) or probucol (10 μM) significantly attenuated Aβ (5 μM, 2 h)-induced decrease in pPKA C level. Densitometry of the pPKA C immunoreactive bands relative to the total PKA C was shown in the indicated groups of cells. The lower panel showed representative immunoblots for pPKA C and total PKA C in the indicated groups. (B) The treatment of antioxidants attenuated Aβ-induced reduction in PKA activity. (C1–C2) Densitometry of the immunoreactive bands for phospho-CREB (pCREB) relative to the total CREB in the indicated groups of cells. Levels of pCREB were increased in cells treated with SOD/catalase (C1) and probucol (C2) in the presence of Aβ. The lower panels in C1 and C2 showed the representative immunoblots for pCREB and total of CREB. Results were derived from 3 to 5 independent experiments.

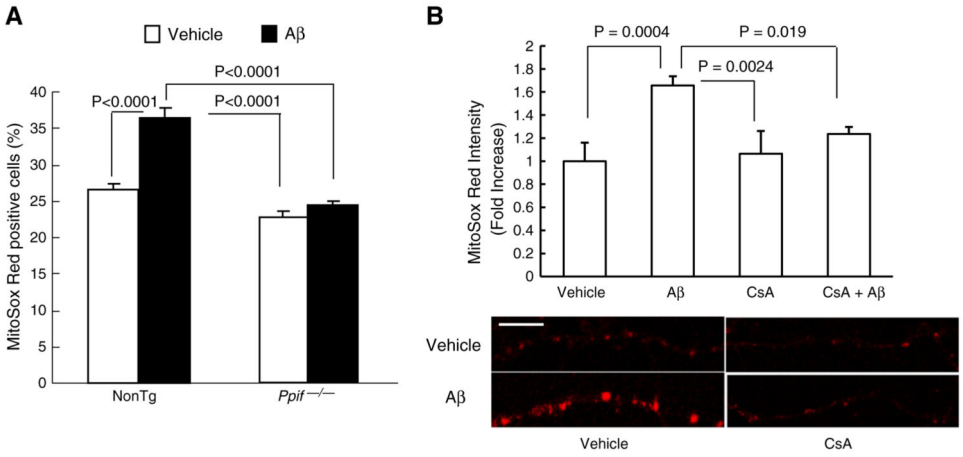

Fig. 2.

Effects of CypD-deficiency on mitochondrial ROS production in neurons exposed to Aβ. (A) Aβ-treated neurons were subjected to MitoSox Red staining and the percentage of MitoSox Red-positive cells was quantified by flow cytometry. (B) CsA treatment significantly attenuated MitoSox Red intensity in Aβ-exposed neurons. Scale bar = 10 μm.

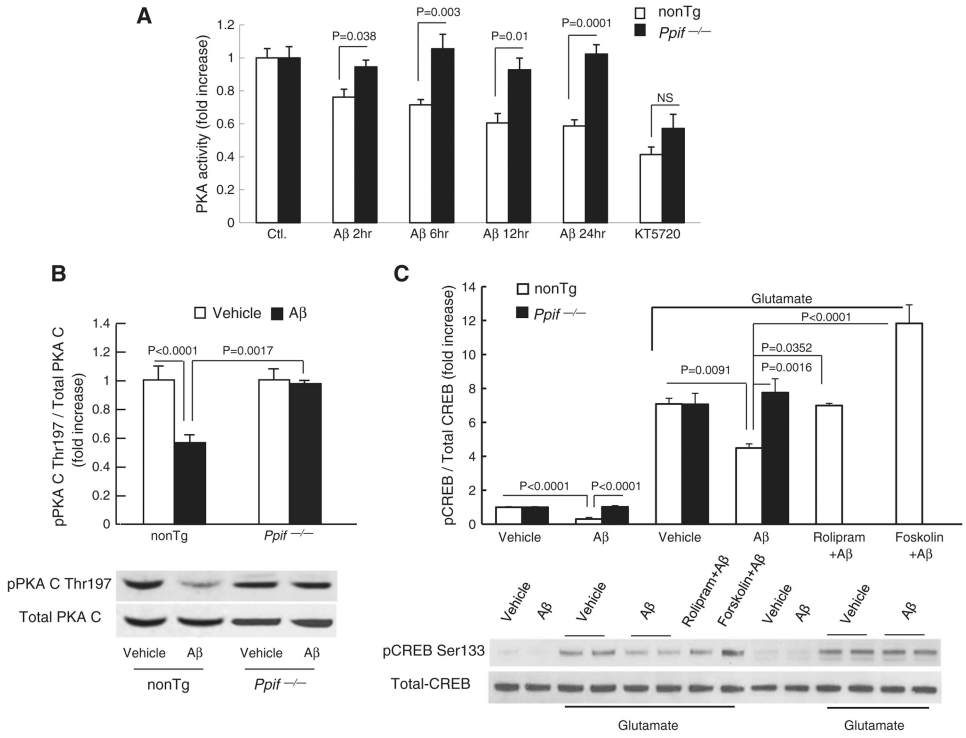

Fig. 3.

Effects of CypD-deficiency on PKA activity, phosphorylation of PKA C (p-PKA C), and pCREB in neurons exposed to Aβ. (A) PKA activity in cultured nonTg and *Ppif*$^{-/-}$ neurons exposed to oligomeric Aβ for 2, 6, 12 and 24 h, respectively. KT5720 (1 μM), a PKA inhibitor, was added to neurons. PKA activity in the indicated cell lysates was determined by PKA Kinase Activity Assay Kit. The data were expressed as fold increased relative to the PKA activity in vehicle-treated nonTg neurons. (B) NonTg and *Ppif*$^{-/-}$ neurons were treated with 5 μM Aβ for 2 h, then subjected to immunoblotting for phosphorylation of PKA C Thr197, and total PKA C. Quantification of intensity of phospho-PKA C immunoreactive bands normalized to total PKA C is presented in the upper panel. The lower panels represent the sample immunoblots for phospho-PKA C Thr197 and PKA C subunit. (C) Effect of CypD deficiency on glutamate-induced phosphorylation of CREB. Cortical neurons were exposed to 5 μM Aβ for 2 h in the presence or absence of glutamate stimulation, and then subjected for immunoblotting for pCREB Ser133 and total CREB. Densitometry of pCREB immunoreactive bands normalized to total CREB is presented in the upper panel and the lower panel shows representative immunoblots for pCREB and CREB. Rolipram (3 μM) and Forskolin (5 μM) were added to cultured neurons.

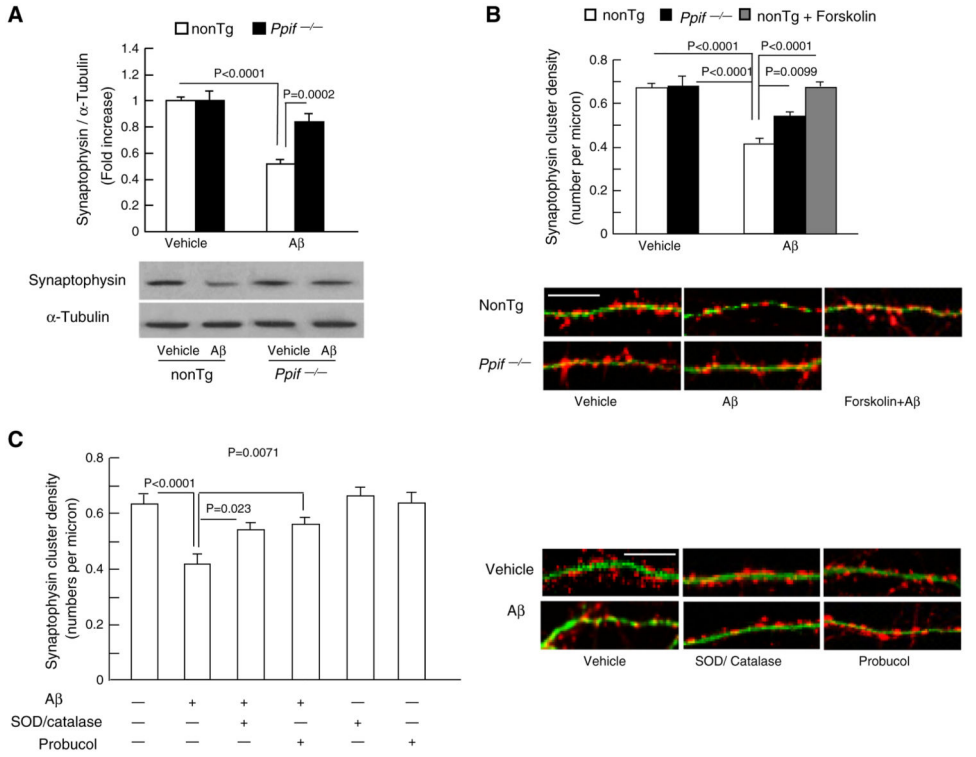

Fig. 4.

Effects of CypD deficiency and antioxidant on Aβ-induced synaptic loss. (A) Expression levels of synaptophysin in Aβ-treated nonTg and *Ppif*$^{-/-}$ neurons. Cultured neurons were treated with 5 μM oligomer Aβ1–42 for 2 h. Cell lysates were subjected to immunoblotting with synaptophysin antibody. Densitometry of the synaptophysin immunoreactive bands was normalized by α-tubulin using NIH Image J software. The lower panels are representative immunoblots for synaptophysin and α-tubulin. Data were collected from 3 to 4 independent experiments. (B) After exposure of 5 μM oligomer Aβ for 2 h, *Ppif*$^{-/-}$ neurons exhibited preserved synaptic positive clusters compared with nonTg neurons. PKA activator, forskolin (5 μ*M),* protected nonTg neurons against Aβ-induced synaptic loss. Data were collected from 17 to 20 neurons per group. The lower panel shows representative images of synaptophysin clusters (synaptophysin, red) and dendrite (MAP2, green) staining. Scale bar = 10 μm. (C) Antioxidants attenuated Aβ-induced synaptic loss. Data are derived from 16 to 23 neurons per group in 3 independent experiments. The right panel shows representative images of synaptic staining. Synapses were visualized by synaptophysin staining (red) and dendrites were shown by MAP2 staining (green). Scale bar = 10 μm.

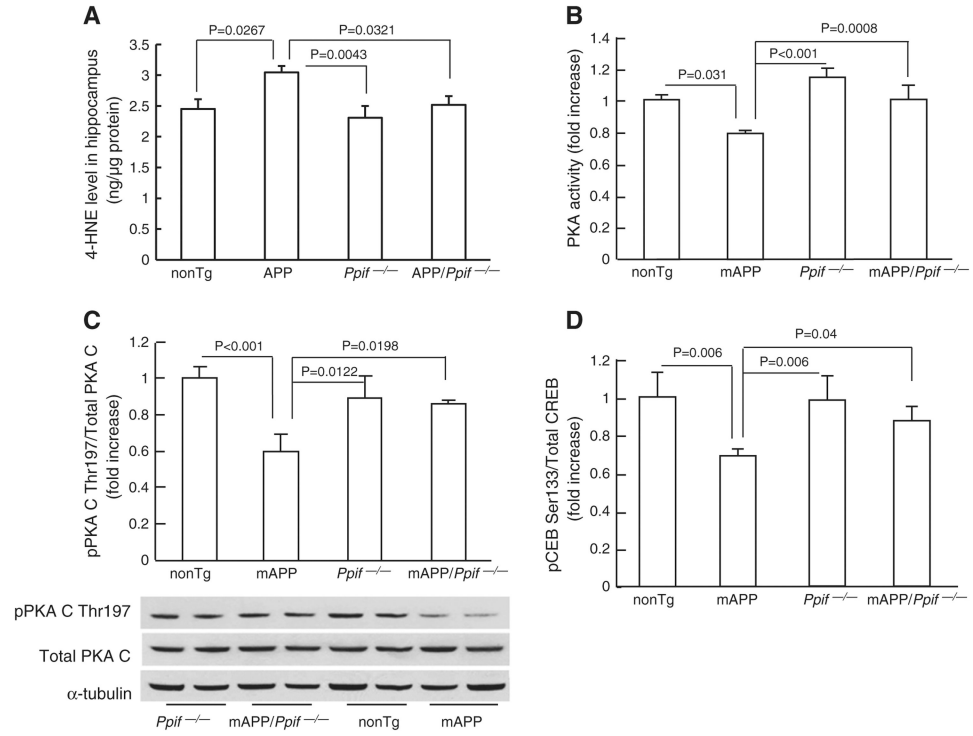

Fig. 5.

Effect of CypD deletion on brain oxidative stress, PKA activity, phosphorylation of PKA C and CREB in mAPP mice. (A) Cerebral cortexes from the indicated Tg mice were subjected to 4-HNE assay. CypD-deficient mAPP mice demonstrated significantly lowered 4-HNE level than mAPP mice. (B) PKA activity in the cerebral cortex of the indicated Tg mice. Data are shown in fold-increase relative to the PKA activity in nonTg mice. (C) Densitometry of immunoreactive bands for p-PKA C, total PKA C, and α-tubulin in the cerebral cortex homogenates of the indicated Tg mice. Data were expressed as fold-increase relative to pPKA C level (normalized to total PKA C) in nonTg mice. The representative immunoblots were demonstrated in lower panel. (D) CREB phosphorylation in Tg mice. Data were shown as fold-increase relative to total CREB.

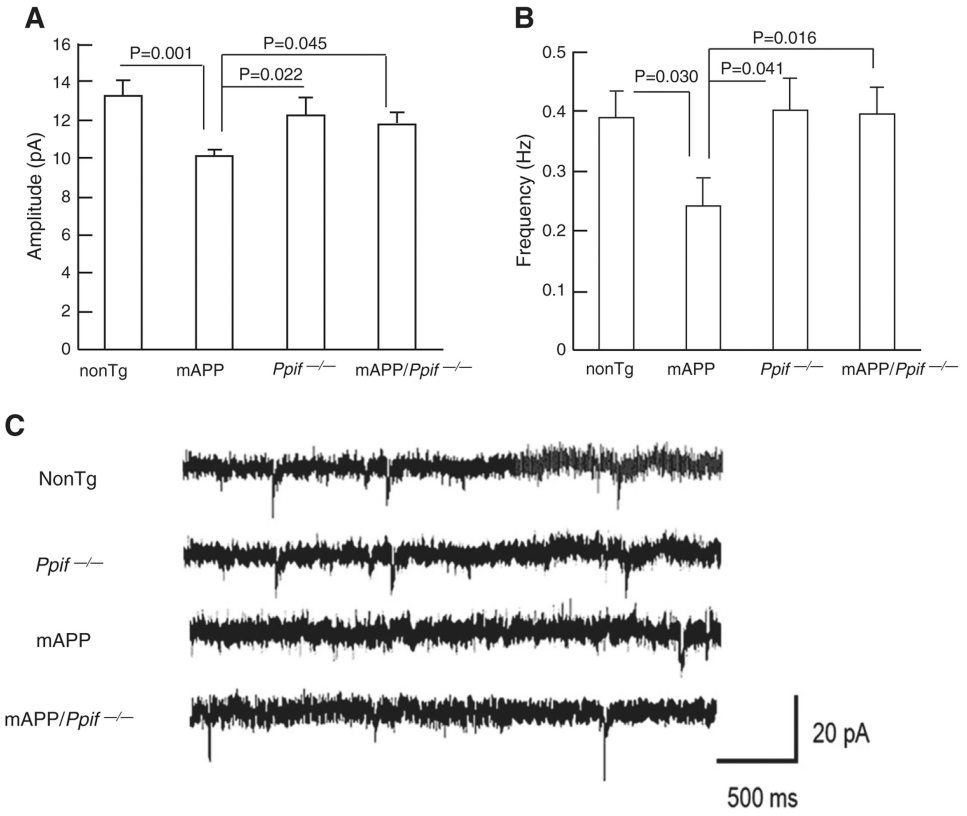

Fig. 6.

Effect of CypD on spontaneous synaptic activity in mAPP mice. mAPP mice showed decreased mEPSC amplitude (A) and frequency (B), which were restored by CypD deficiency. (C) The representative traces of mEPSC recorded for CA1 neurons from the indicated Tg mice. Scale = 20 pA, 500 ms.

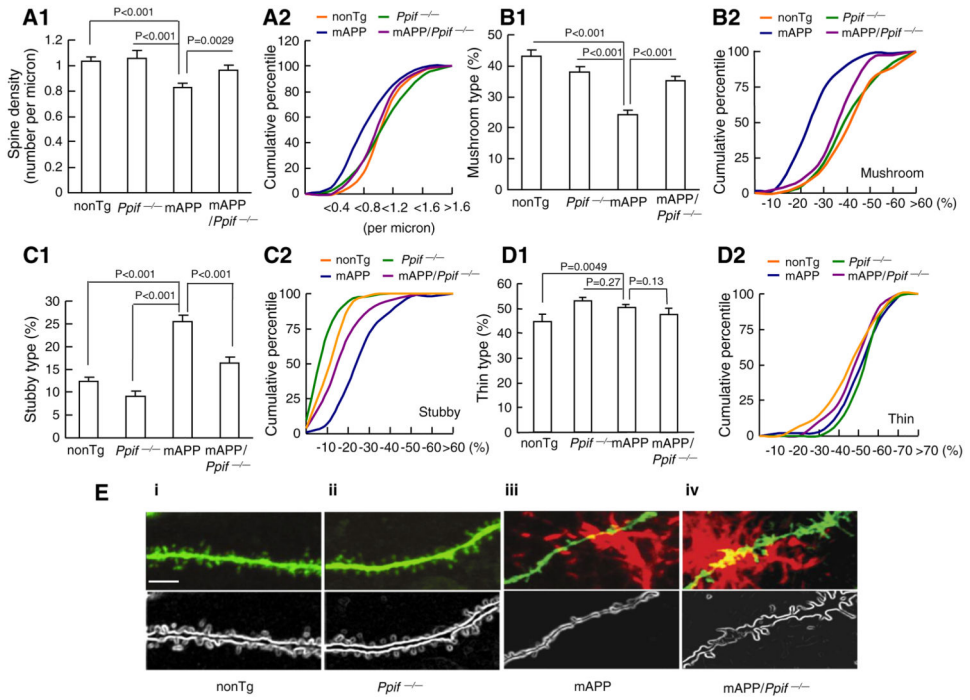

Fig. 7.

Effect of CypD deletion on dendritic spine architecture in mAPP mice. (A–D) Quantification of spine density (A) and types of synaptic morphology (B–D). (A) The comparison of spine density. N = 4–6 mice per group, 10, 11, 15 and 12 neurons from nonTg, *Ppif*$^{-/-}$, mAPP mice, and mAPP/*Ppif*$^{-/-}$ mice, respectively. (B–D) The comparison of the percentage of mushroom (B1–2), stubby (C1–2), and thin (D1–2) type spines occupied by the total dendritic spines. (E) Representative images of basal dendritic spines of CA1 neurons in Tg mice. Dendritic spines (green) and senile plaques (red) were visualized by Lucifer yellow injection and 3D6 immunostaining, respectively. The panels i, ii, iii and iv show representative images of dendritic spines from nonTg, *Ppif*$^{-/-}$, mAPP and mAPP/*Ppif*$^{-/-}$ mice, respectively. The lower panels present outlines of the dendritic spines corresponding to the images above. Scale bar = 5 μm.

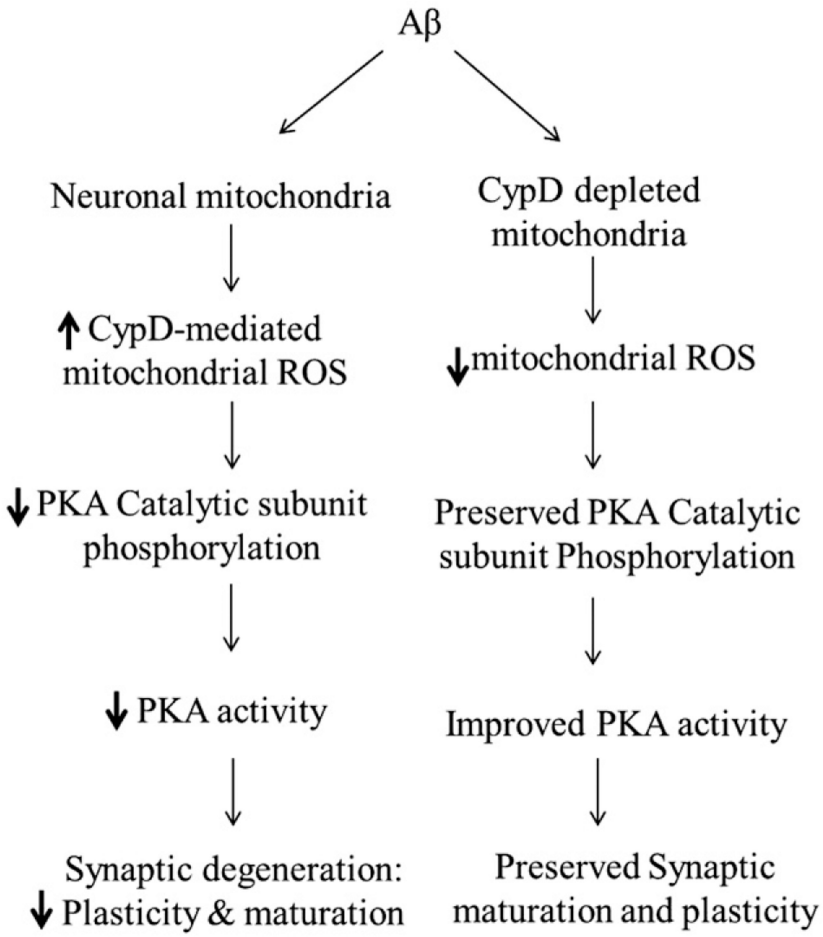

Fig. 8.

Schematic figure of CypD deficiency protects synaptic plasticity and maturation against Aβ toxicity. In the presence of CypD, Aβ augments mitochondrial ROS production/ accumulation, subsequently decreases phosphorylation of PKA catalytic subunit and the resultant depression in PKA/CREB signaling transduction, eventually leading to synaptic degeneration. In contrast, the deficiency of CypD attenuates Aβ-instigated mitochondrial ROS production and thereby ameliorates PKA/CREB perturbation and improves synaptic plasticity and maturation in Aβ rich scenario.